



OPEN

Chromosome-level genome assembly of *Salvia sclarea*

DATA DESCRIPTOR

Sehyun Choi¹, Yuna Kang¹ & Changsoo Kim^{1,2}✉

Salvia sclarea is a medicinal herb from the Lamiaceae family, valued for its essential oil which contains sclareol, linalool, linalyl acetate, and other compounds. Despite its extensive use, the genetic mechanisms of *S. sclarea* are not well understood. This study presents a chromosome-level genome assembly of *S. sclarea* using the Oxford Nanopore Technology, Illumina short reads, and Pore-C technology. The assembled genome spans 499.03 Mbp with a scaffold N50 of 50.5 Mbp, forming 11 pseudochromosomes. The genome assembly was validated by BUSCO analysis, which indicated a high completeness marked at 98.7%. The genome contains 68.73% repetitive sequences, with long terminal repeats (LTRs) accounting for 33.01%. A total of 17,202 protein-coding genes were predicted. Among them, 16,846 genes were annotated in the NCBI NR database, the highest among all databases, covering 97.93% of the predicted genes. The phylogenetic analysis revealed that *S. sclarea* shares a close evolutionary relationship with *S. officinalis* within the *Salvia* genus, while species in the genus have evolved independently within the Lamiaceae family. This high-resolution genome assembly offers fresh insights into the biosynthesis of essential oils and other aromatic compounds in *S. sclarea*, establishing a basis for genetic preservation.

Background & Summary

Salvia sclarea, commonly known as clary sage, is an herbaceous plant belonging to the *Salvia* genus within the Lamiaceae family. Native to the Mediterranean region, this plant is now cultivated in various parts of the world and can be biennial or perennial¹. Clary sage has been used for centuries due to its medicinal properties. The oil extracted from the flowers and leaves of *S. sclarea* has been utilized in traditional medicine for its anti-inflammatory, antimicrobial, and antioxidant properties^{2,3}. Beyond its medicinal value, the essential oil is used in the cosmetics industry, particularly in perfumes. The main components of *S. sclarea* essential oil include linalool, linalyl acetate, geraniol, nerol, neryl acetate, and sclareol^{4,5}.

The significance of *S. sclarea* extends beyond its traditional uses, with its essential oils highly valued in various industries. Recently, pseudochromosome-level genome studies have been published for various plants within the *Salvia* genus, such as *S. splendens*, *S. miltiorrhiza*, and *S. hispanica*^{6–8}. Despite its extensive use and research into its medicinal and aromatic properties, the genetic basis of these traits in *S. sclarea* has not been fully explored.

This study generated a chromosome-level genome assembly of *S. sclarea* using Oxford Nanopore Technology (ONT) long reads, Illumina short reads (NGS), and Pore-C technology. A total of 499.03 Mbp genome was assembled with a scaffold N50 length of 50.5 Mbp. Furthermore, 11 pseudo-chromosomes were generated by integrating the Pore-C data. This chromosome-scale genome provides new insights into the biosynthesis of important aromatic compounds, such as essential oils in *S. sclarea*, and lays the foundation for genetic conservation. Additionally, the genome assembly will facilitate future research to improve clary sage through genetic breeding and biotechnological approaches, ultimately enhancing its economic and medicinal value.

Methods

Sample preparation. The seeds of *S. sclarea* for the new genome assembly were obtained from a garden center in Yangpyeong, South Korea. The plants were germinated under controlled conditions with a 12-hour light/dark cycle, maintaining temperatures at 26 °C during the day and 28 °C at night. Young leaf samples were collected at the seedling stage and stored at –80 °C. High molecular weight genomic DNA was extracted using the CTAB⁹ method, and DNA fragments smaller than 10 kb or 25 kb were removed using the Short Read Eliminator (SRE) kit from Circulomics. The genomic DNA was further purified and concentrated using AMPure XP beads

¹Department of Crop Science, Chungnam National University, Daejeon, 34134, Korea. ²Department of Science in Smart Agriculture Systems, Chungnam National University, Daejeon, 34134, Korea. ✉e-mail: changsookim@cnu.ac.kr

Library type	Platform	Data size (Gb)	Coverage(X)	Read length (bp)
WGS short reads	Illumina Novaseq6000	54.4	108	150
WGS long reads	Nanopore PromethION	28.23	56	38491 (N50)
Pore-C	Nanopore PromethION	58.83	116	150
RNA-Seq	Illumina Novaseq6000	8.8	—	150

Table 1. Summary of sequencing data for *Salvia sclarea*.

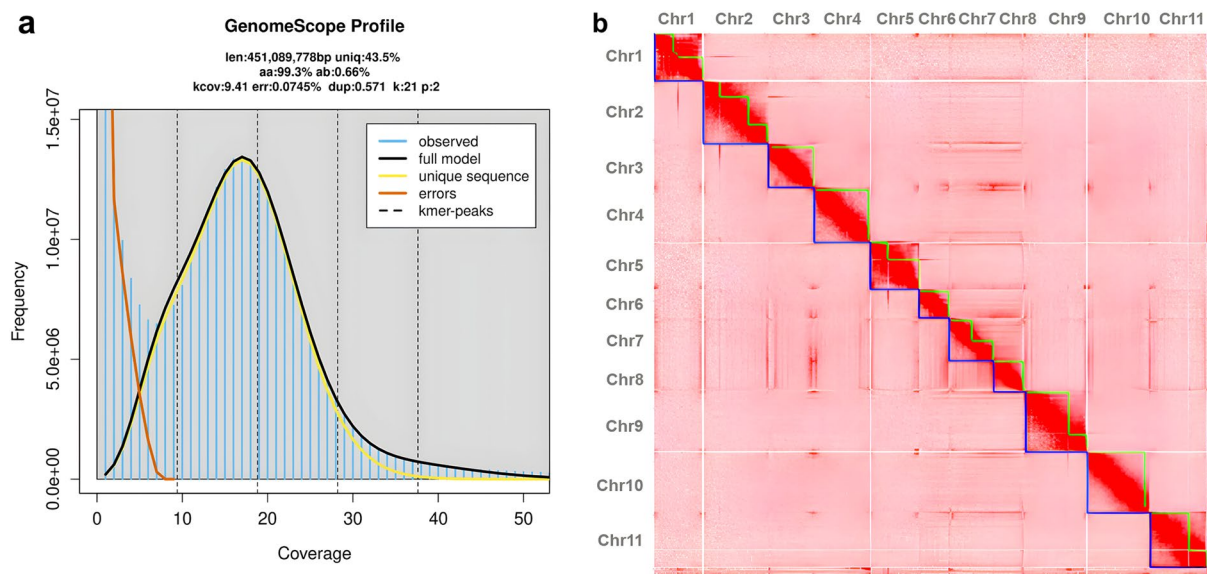


Fig. 1 Chromosome-Level Genome Assembly of *Salvia sclarea* (a) K-mer analysis of *S. sclarea* genome using GenomeScope profile (b) Pore-C interaction Heatmap illustrating chromosomal interactions in the *S. sclarea* genome.

(Beckman Coulter). The DNA concentration and purity were measured with a NanoDrop spectrophotometer and Qubit fluorometer.

Genome and transcriptome sequencing. The sequencing library for Oxford Nanopore Technology (ONT) was prepared using the SQK-LSK114 ONT kit. ONT sequencing was performed on a PromethION sequencer using FLO-PRO114M flow cells, generating a total of 28.23 GB (56x) of raw genomic data (Table 1). The samples sequenced on the PromethION platform were processed using ONT's Guppy (v6.5.7) software to convert the raw ONT sequencing data (FAST5 files) into FASTQ format.

For the short-read sequencing library, DNA was extracted using the Plant DNA(III) extraction kit (SmartGene, Korea) and prepared with the Illumina TruSeq DNA Nano library preparation kit (Illumina, San Diego, CA, USA). Paired-end sequencing was carried out on the Illumina NovaSeq6000 platform, producing 54.4 GB (108x) of raw data (Table 1).

Total RNA was extracted from the same leaves used for the genome analysis using the Plant RNA extraction kit (SmartGene, Korea). The RNA library was then constructed with the TruSeq Stranded mRNA kit (Illumina, San Diego, CA, USA) and sequenced on the Illumina NovaSeq6000 platform, producing 8.8 Gb of raw RNA data (Table 1).

Sequencing and *De novo* assembly of the Pore-C data. We performed a k-mer analysis using Jellyfish (v2.3.1)¹⁰ with a k-mer size of 21. The k-mer frequency distribution was then analyzed using GenomeScope (v2.0)¹¹. The x-axis shows the coverage, and the y-axis shows the k-mer frequency. Observed data are in blue; the model fit is in yellow; unique sequences are in orange, and error sequences are in green. Key metrics include a genome length of 451,089,778 bp, with 43.5% unique sequences, a heterozygosity of 0.66%, an error rate of 0.074%, and a duplication rate of 0.571%. This analysis estimated the genome size to be 451.08 Mb (Fig. 1a).

The Pore-C raw data for *S. sclarea* were generated using the PromethION platform. The raw data were processed using Guppy (v6.5.7) from ONT to produce fastq files with a Phred quality score of ≥ 7 , ensuring high-quality sequencing reads. The resulting fastq files were approximately 58.83 GB (116x) in size (Table 1). The resulting fastq files were then subjected to statistical analysis using NanoPlot (v1.41.6)¹² to evaluate the data quality and distribution. The Pore-C data was assembled using NextDenovo (v2.5.2)¹³, which efficiently

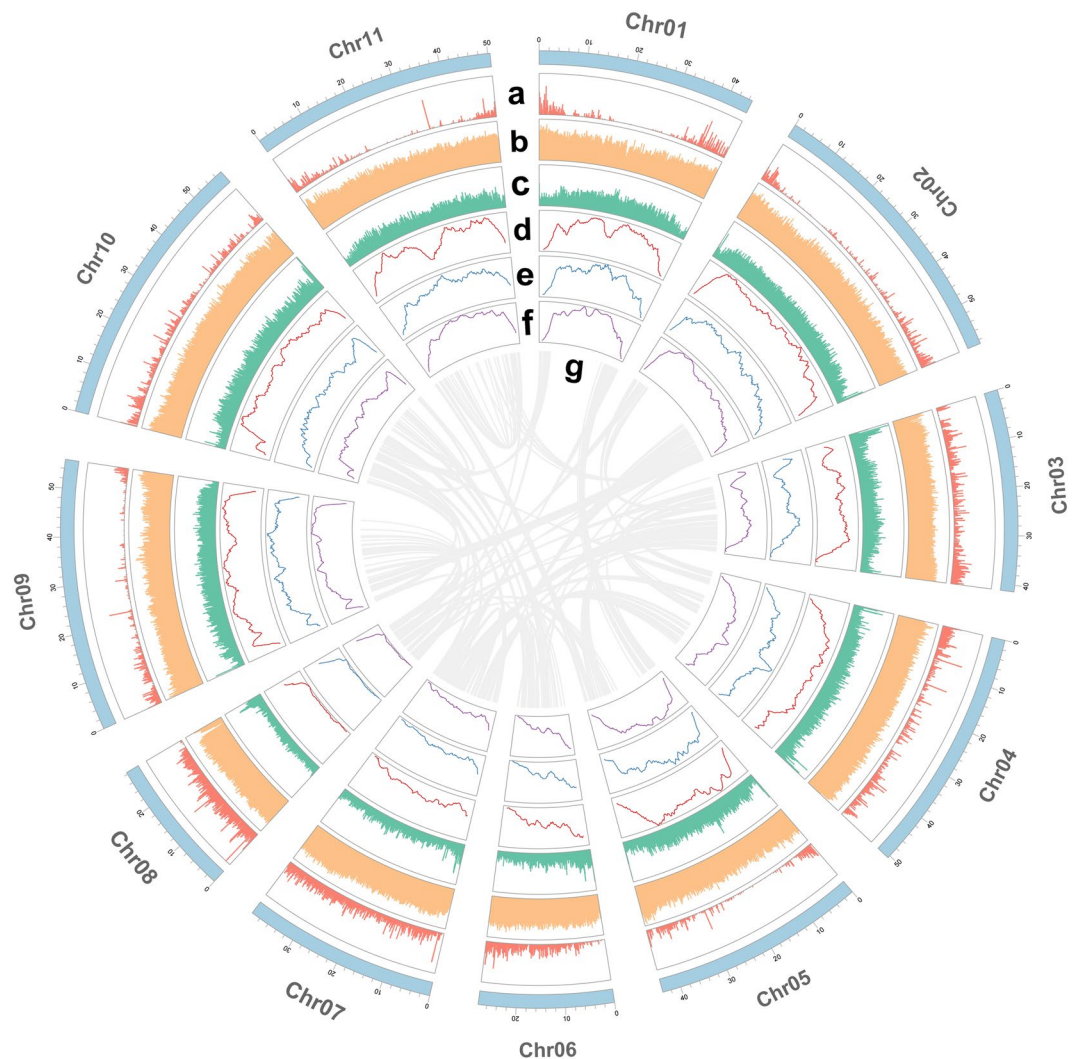


Fig. 2 Circos plot of the genomic landscape of *S. sclarea*. **(a)** Gene density. **(b)** Repeat sequences density. **(c)** GC content. **(d)** Copia density. **(e)** Gypsy density. **(f)** LTR density **(g)** Intraspecies collinearity.

assembled the sequencing reads into contiguous sequences. The preliminary assembly was then polished using NextPolish (v1.4.1)¹⁴ to improve the accuracy and quality of the assembled sequences.

Genome scaffolding was performed using the YaHS-1.1¹⁵ tool with the Pore-C data. First, contig sequences in the FASTA format were indexed with Samtools (v1.20)¹⁶. The Pore-C reads were aligned to these contigs, resulting in a sorted and duplicate-marked BAM file. YaHS was then run with the contig and BAM files to generate scaffolded assemblies, producing AGP and FASTA outputs. Visualization and manual curation of Pore-C contact maps were conducted using JuicerTools (v3.0)¹⁷ and Juicebox (v2.20.00)¹⁸, ensuring the accuracy of the scaffolding.

The Pore-C interaction heatmap visually represents the interaction data across the 11 chromosomes of *S. sclarea*. The x-axis and y-axis denote chromosomes, with each cell showing the interaction frequency between the genomic regions. The heatmap confirms the assembly's accuracy, showing distinct chromosomes with minimal cross-chromosomal interactions, validating the high-quality chromosome-level genome assembly (Fig. 1b).

Chromosome-level genome assembly. Previous studies have confirmed that *S. sclarea* has a diploid chromosome number of $2n = 2x = 22$ ^{19–21}. The distribution of various genomic features across the 11 chromosomes was visualized using TBtools²². The circos plot presents various genomic features of *S. sclarea* across its 11 pseudochromosomes (Fig. 2a). The outermost ring shows the gene density, followed by the repeat sequence density in the second ring. The third ring displays the GC content, while the fourth and fifth rings show the Copia and Gypsy element densities, respectively. The sixth ring highlights the overall LTR density. The innermost lines represent chromosomal synteny within the *S. sclarea* genome. These visualizations provide detailed insights into the genomic architecture and repeat element composition.

The assembly includes 72 scaffolds that were organized into 11 pseudochromosomes. These pseudochromosomes were refined and finalized through manual curation utilizing Pore-C interaction heatmaps, which

Final statistics of Pore-C scaffolding	
The number of scaffolds (pseudomolecule)	11
Total scaffolds number	72
Total contigs number	112
Total length	499,032,627 bp
Total length of unscaffolded contig	7,653,700 bp
Minimum length of scaffold	27,721,853 bp
Maximum length of scaffold	58,827,749 bp
Scaffold N50	50,476,100 bp
Scaffold N90	28,402,000 bp
Contig N50	26,293,000 bp
Contig N90	15,270,000 bp
Number of scaffolds > 50 KB	55
% main genome in scaffolds > 50 KB	99.90%

Table 2. Genome assembly and annotation statistics of *S. sclarea* using Pore-C scaffolding.

ID	Length (bp)
Chr1	44725600
Chr2	58827749
Chr3	41332168
Chr4	50521182
Chr5	43770601
Chr6	27721853
Chr7	39891702
Chr8	28402147
Chr9	55812712
Chr10	57550813
Chr11	50476100
Total	499032627

Table 3. The assembly of *S. sclarea* resulted in 11 pseudochromosomes with lengths.

Type	Count	Ratio(%)
Complete BUSCOs (C)	1593	98.7%
Complete and single-copy BUSCOs (S)	1554	96.3%
Complete and duplicated BUSCOs (D)	39	2.4%
Fragmented BUSCOs (F)	10	0.6%
Missing BUSCOs (M)	11	0.7%
Total BUSCO groups searched	1614	100%

Table 4. Result of the BUSCO assessment of *S. sclarea*.

ensured accurate chromosomal mapping. The final genome assembly spans 499.03 Mb, with a scaffold N50 value of 50.47 Mb, reflecting a high degree of continuity and assembly quality (Table 2). The lengths of the pseudochromosomes range from 27.72 Mb to 58.83 Mb, totaling 499.03 Mb (Table 3).

Assessing genomic data. To assess the completeness of the *S. sclarea* genome assembly, we employed the BUSCO (Benchmarking Universal Single-Copy Orthologs) v5.4.3²³ tool. Using the embryophyta_odb10 database, the analysis evaluated the presence of single-copy orthologs. The results indicated a high level of completeness, with 98.7% of the orthologs being complete (single-copy: 96.3%, duplicated: 2.4%). Only 0.6% of the orthologs were fragmented, and 0.7% were missing. These findings confirm the robustness and quality of the genome assembly (Table 4).

Repeat annotation and LTR insertion. To annotate repetitive elements in the *S. sclarea* genome, we used a combination of RepeatModeler (v2.0.1)²⁴ and RepeatMasker (v4.1.2-pl)²⁵. Initially, RepeatModeler was used to identify and classify *de novo* repeat families. Subsequently, RepeatMasker utilized this repeat library to mask and annotate the repetitive sequences within the genome. The genome of *S. sclarea* contains a significant proportion of repetitive elements, comprising 68.73% of the total sequence. Retroelements occupy 33.63% of the genome, with LTR elements being the most prominent at 33.01%. Ty1/Copia elements account for 21.72%, and Gypsy/

	Number of elements	Length occupied	Percentage of sequence
Retroelements	63707	167835296 bp	33.63%
SINEs:	0	0 bp	0.00%
Penelope:	0	0 bp	0.00%
LINEs:	3266	3106031 bp	0.62%
CRE/SLACS	0	0 bp	0.00%
L2/CR1/Rex	0	0 bp	0.00%
R1/LOA/Jockey	0	0 bp	0.00%
R2/R4/NeSL	0	0 bp	0.00%
RTE/Bov-B	0	0 bp	0.00%
L1/CIN4	3266	3106031 bp	0.62%
LTR elements:	60441	164729265 bp	33.01%
BEL/Pao	0	0 bp	0.00%
Ty1/Copia	32442	108414020 bp	21.72%
Gypsy/DIRS1	26971	53911254 bp	10.80%
Retroviral	0	0 bp	0.00%
DNA transposons	15170	8480073 bp	1.70%
hobo-Activator	2655	844031 bp	0.17%
Tc1-IS630-Pogo	1490	709657 bp	0.14%
En-Spm	0	0 bp	0.00%
MULE-MuDR	4813	3245267 bp	0.65%
PiggyBac	0	0 bp	0.00%
Tourist/Harbinger	4019	2031296 bp	0.41%
Other (Mirage,	0	0 bp	0.00%
P-element, Transib)			
Rolling-circles	4743	2373257 bp	0.48%
Unclassified:	425389	158507734 bp	31.76%
Total interspersed repeats:		334823103 bp	67.09%
Small RNA:	0	0 bp	0.00%
Satellites:	0	0 bp	0.00%
Simple repeats:	111375	5117419 bp	1.03%
Low complexity:	13741	676966 bp	0.14%
Total		342990745 bp	68.73%

Table 5. Annotation of repeat elements in *S. sclarea*.

DIRS1 elements account for 10.80% of the genome. DNA transposons make up 1.70% of the genome. In total, interspersed repeats account for 67.09% of the genome (Table 5).

For the identification of long terminal repeat (LTR) retrotransposons, we implemented a two-step approach. First, LTR candidates were detected using LTR-finder (v1.1)²⁶ and LTR-harvest²⁷ as part of the GenomeTools (v1.6.5)²⁸ package. The results from these tools were then integrated and refined using LTR-retriever (v2.9.0)²⁹, which provided a comprehensive and accurate annotation of LTR elements.

The insertion time of these LTR elements was analyzed to provide insights into their evolutionary history within the genome. Using the density plot for insertion times, we identified the insertion periods for various LTR types: Copia elements showed a peak insertion time at approximately 0.02 million years ago (MYA), Gypsy elements at 0.04 MYA, and unknown elements at 0.01 MYA (Fig. 3).

Gene annotation. Gene annotation for the *S. sclarea* genome was performed using a combination of ab initio prediction, homology-based methods, and transcriptome data. For the ab initio gene prediction, we used Braker2 (v2.1.6)³⁰ and SNAP³¹. Braker2 utilizes RNA-seq data to train the gene prediction models, while SNAP is used to refine the predictions. Homology-based annotation was conducted using GeMoMa (v1.8)³². For this purpose, we utilized genome data from closely related species available in the NCBI database, specifically *Salvia splendens*, *Salvia hispanica*, *Salvia miltiorrhiza*, and *Salvia rosmarinus*. RNA-seq reads were assembled using StringTie (v2.1.4)³³, which provided transcript assemblies used as evidence for gene prediction. Furthermore, we utilized Trinity (v2.15.1)³⁴ to assemble RNA-seq data into contigs, and these were processed with TransDecoder (v5.7.1)³⁵ to identify candidate coding regions within the assembled transcripts. Finally, predictions from ab initio methods, homology-based approaches, and transcriptome evidence were integrated using EVidenceModeler (EVM) v2.1.036³⁶.

Functional annotation of genes was conducted using a two-pronged approach. Protein sequences were aligned against the NCBI non-redundant protein (NR)³⁷ database and the Swiss-prot³⁸ database utilizing DIAMOND (v2.1.9)³⁹, ensuring efficient sequence alignment. EggNOG-mapper⁴⁰ was used to annotate protein sequences, leveraging the Kyoto Encyclopedia of Genes and Genomes (KEGG)⁴¹, Gene Ontology (GO)⁴² terms,

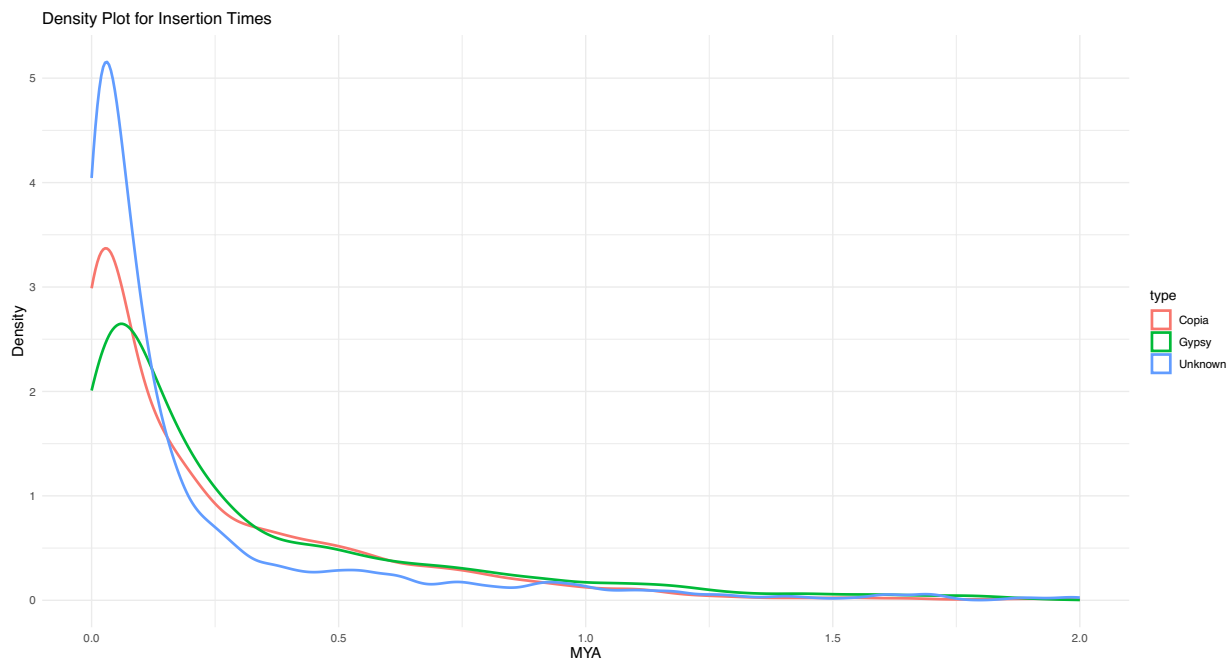


Fig. 3 Density plot for LTR retrotransposon insertion times in *S. sclarea*: Distribution of Copia, Gypsy, and Unknown elements.

Genome annotation	Number of elements
Predicted protein-coding genes	17202
Uniprot	16797
NCBI NR	16846
eggNOG	16251
KEGG	8409
GO	8576
Pfam	14596

Table 6. Functional annotation of *S. sclarea* genes.

and Pfam⁴³ to provide comprehensive functional insights. The NCBI NR database annotated 16,846 genes, the highest among all databases, covering 97.93% of the 17,202 predicted genes (Table 6).

The Venn diagram shows the overlaps and unique counts of functionally annotated genes in *S. sclarea* across five databases. Uniprot contains 16,797 gene annotations, while NCBI NR has 16,846 gene annotations. EggNOG includes 16,251 annotated genes, with GO covering 8,576 annotations and KEGG 8,409 annotations, while Pfam annotates 14,596 genes. The central overlapping area shows 5,660 gene annotations common across all five databases. Overlaps include 1,840 annotations shared between Uniprot and NCBI NR, and 3,686 annotations shared between NCBI NR and Pfam. This visualization represents the distribution and intersection of gene annotations across multiple databases (Fig. 4).

Phylogenetic analysis in lamiaceae. Phylogenetic tree was constructed to identify the evolutionary relationships between *S. sclarea* and eight other species based on single-copy genes using OrthoVenn3⁴⁴. Three species from the family Lamiaceae were included: *Hyssopus officinalis* (datadryad.org/stash/dataset/doi:10.5061/dryad.88tj450), *Nepeta cataria* (datadryad.org/stash/dataset/doi:10.5061/dryad.88tj450), *Nepeta mussinii* (datadryad.org/stash/dataset/doi:10.5061/dryad.88tj450). And five species from the genus *Salvia* were included: *Salvia splendens* (GCF_004379255.2), *Salvia hispanica* (GCF_023119035.1), *Salvia divinorum* (GCA_041381175.1), *Salvia miltiorrhiza* (GCF_028751815.1), and *Salvia officinalis*⁴⁵, which were obtained from NCBI database (<http://www.ncbi.nlm.nih.gov/>). Muscle⁴⁶ was used to align the sequences, trimAl⁴⁷ was used to extract and trim the conserved sequences, and FastTree⁴⁸ was used to construct a phylogenetic tree based on the maximum likelihood method. The analysis was performed using the JTT + CAT model, and the reliability of each node was assessed by the SH test method. Each branch point is indicated with a confidence level of 100, which confirms that the structure of the phylogenetic tree has high statistical reliability.

independently within the Lamiaceae, which provides important information for understanding genetic diversity and evolutionary relationships.

Data Records

The genomic sequencing data (Illumina, Nanopore, Pore-C) are available in the NCBI SRA database, with specific accession numbers as follows: SRP510693⁴⁹, with specific accession numbers as follows:

The Pore-C sequencing data were deposited in the Sequence Read Archive at the NCBI (SRX24744566)⁵⁰.

The genomic Nanopore sequencing data were deposited in the Sequence Read Archive at the NCBI (SRX24744567)⁵¹.

The genomic Illumina sequencing data were deposited in the Sequence Read Archive at the NCBI (SRX24744565)⁵².

The transcriptome Illumina sequencing data were deposited in the Sequence Read Archive at the NCBI (SRX24744564)⁵³.

The final chromosome assembly was deposited in GenBank at the NCBI (GCA_041430365.1)⁵⁴.

The genome annotation files, including predicted CDS and protein sequences and GFF files, are available in the FigShare database (<https://doi.org/10.6084/m9.figshare.27002593.v1>)⁵⁵.

Technical Validation

The final DNA extracted using the CTAB method and purified with the SRE kit for Nanopore sequencing was analyzed for length and quality using gel electrophoresis and the TapeStation 2200 before proceeding with library preparation.

Code availability

Nanopore Pore-C Data. These mnd files, along with the initial assembly results, were input into the 3d-dna pipeline (v180922) using the run-asm-pipeline.sh script with the following options: -i 10000 --polisher-input-size 1000000 --splitter-input-size 1000000 -r 2 --editor-coarse-resolution 250000 --editor-coarse-region 1250000 -q 0 --polisher-coarse-resolution 1000000 --polisher-coarse-region 30000000. This process generated the rawchrom. assembly, rawchrom.hic, and FINAL.fasta files.

Received: 18 September 2024; Accepted: 19 December 2024;

Published online: 04 January 2025

References

- Aćimović, M. G. *et al.* Biological activity and profiling of *Salvia sclarea* essential oil obtained by steam and hydrodistillation extraction methods via chemometrics tools. *Flavour and Fragrance Journal* **37**, 20–32 (2022).
- Gülçin, I., UĞUZ, M. T., Oktay, M., Beydemir, Ş. & Küfrevioğlu, Ö. İ. Evaluation of the antioxidant and antimicrobial activities of clary sage (*Salvia sclarea* L.). *Turkish Journal of Agriculture and Forestry* **28**, 25–33 (2004).
- Peana, A. T., Moretti, M. D. & Juliano, C. Chemical composition and antimicrobial action of the essential oils of *Salvia desoleana* and *S. sclarea*. *Planta medica* **65**, 752–754 (1999).
- Pitarokili, D., Couladis, M., Petsikos-Panayotou, N. & Tzakou, O. Composition and antifungal activity on soil-borne pathogens of the essential oil of *Salvia sclarea* from Greece. *Journal of agricultural and food chemistry* **50**, 6688–6691 (2002).
- Hristova, Y. *et al.* Chemical composition and antifungal activity of essential oil of *Salvia sclarea* L. from Bulgaria against clinical isolates of *Candida* species. *Journal of BioScience & Biotechnology* **2** (2013).
- Wang, L. *et al.* A chromosome-level genome assembly of chia provides insights into high omega-3 content and coat color variation of its seeds. *Plant Communications* **3** (2022).
- Pan, X. *et al.* Chromosome-level genome assembly of *Salvia miltiorrhiza* with orange roots uncovers the role of Sm2OGD3 in catalyzing 15, 16-dehydrogenation of tanshinones. *Horticulture Research* **10**, uhad069 (2023).
- Jia, K.-H. *et al.* Chromosome-scale assembly and evolution of the tetraploid *Salvia splendens* (Lamiaceae) genome. *Horticulture Research* **8** (2021).
- Doyle, J. J. & Doyle, J. L. A rapid DNA isolation procedure for small quantities of fresh leaf tissue. *Phytochemical bulletin* (1987).
- Marçais, G. & Kingsford, C. A fast, lock-free approach for efficient parallel counting of occurrences of k-mers. *Bioinformatics* **27**, 764–770 (2011).
- Vurtture, G. W. *et al.* GenomeScope: fast reference-free genome profiling from short reads. *Bioinformatics* **33**, 2202–2204 (2017).
- De Coster, W., D’hert, S., Schultz, D. T., Cruts, M. & Van Broeckhoven, C. NanoPack: visualizing and processing long-read sequencing data. *Bioinformatics* **34**, 2666–2669 (2018).
- Hu, J. *et al.* NextDenovo: an efficient error correction and accurate assembly tool for noisy long reads. *Genome Biology* **25**, 107 (2024).
- Hu, J., Fan, J., Sun, Z. & Liu, S. NextPolish: a fast and efficient genome polishing tool for long-read assembly. *Bioinformatics* **36**, 2253–2255 (2020).
- Zhou, C., McCarthy, S. A. & Durbin, R. YaHS: yet another Hi-C scaffolding tool. *Bioinformatics* **39**, btac808 (2023).
- Li, H. *et al.* The sequence alignment/map format and SAMtools. *Bioinformatics* **25**, 2078–2079 (2009).
- Durand, N. C. *et al.* Juicebox provides a one-click system for analyzing loop-resolution Hi-C experiments. *Cell systems* **3**, 95–98 (2016).
- Durand, N. C. *et al.* Juicebox provides a visualization system for Hi-C contact maps with unlimited zoom. *Cell systems* **3**, 99–101 (2016).
- Muravenko, O. V. *et al.* Integration of Repeatomic and Cytogenetic Data on Satellite DNA for the Genome Analysis in the Genus *Salvia* (Lamiaceae). *Plants* **11**, 2244, <https://doi.org/10.3390/plants11172244> (2022).
- Kharazian, N. Karyotypic study of some *Salvia* Lamiaceae species from Iran. *Journal of applied biological sciences* **5**, 21–25 (2011).
- Özdemir, C. & Şenel, G. The Morphological, Anatomical and Karyological Properties of *Salvia sclarea* L. *Turkish Journal of Botany* **23**, 7–18 (1999).
- Chen, C. *et al.* TBtools: an integrative toolkit developed for interactive analyses of big biological data. *Molecular plant* **13**, 1194–1202 (2020).
- Simão, F. A., Waterhouse, R. M., Ioannidis, P., Kriventseva, E. V. & Zdobnov, E. M. BUSCO: assessing genome assembly and annotation completeness with single-copy orthologs. *Bioinformatics* **31**, 3210–3212 (2015).
- Flynn, J. M. *et al.* RepeatModeler2 for automated genomic discovery of transposable element families. *Proceedings of the National Academy of Sciences* **117**, 9451–9457 (2020).

25. Tempel, S. Using and understanding RepeatMasker. *Mobile genetic elements: protocols and genomic applications*, 29–51 (2012).
26. Xu, Z. & Wang, H. LTR_FINDER: an efficient tool for the prediction of full-length LTR retrotransposons. *Nucleic acids research* **35**, W265–W268 (2007).
27. Ellinghaus, D., Kurtz, S. & Willhoeft, U. LTRharvest, an efficient and flexible software for *de novo* detection of LTR retrotransposons. *BMC bioinformatics* **9**, 1–14 (2008).
28. Gremme, G., Steinbiss, S. & Kurtz, S. GenomeTools: a comprehensive software library for efficient processing of structured genome annotations. *IEEE/ACM transactions on computational biology and bioinformatics* **10**, 645–656 (2013).
29. Ou, S. & Jiang, N. LTR_retriever: a highly accurate and sensitive program for identification of long terminal repeat retrotransposons. *Plant physiology* **176**, 1410–1422 (2018).
30. Brůna, T., Hoff, K. J., Lomsadze, A., Stanke, M. & Borodovsky, M. BRAKER2: automatic eukaryotic genome annotation with GeneMark-EP+ and AUGUSTUS supported by a protein database. *NAR genomics and bioinformatics* **3**, lqaa108 (2021).
31. Korf, I. Gene finding in novel genomes. *BMC bioinformatics* **5**, 1–9 (2004).
32. Keilwagen, J., Hartung, F., Paulini, M., Twardziok, S. O. & Grau, J. Combining RNA-seq data and homology-based gene prediction for plants, animals and fungi. *BMC bioinformatics* **19**, 1–12 (2018).
33. Pertea, M. *et al.* StringTie enables improved reconstruction of a transcriptome from RNA-seq reads. *Nature biotechnology* **33**, 290–295 (2015).
34. Grabherr, M. G. *et al.* Full-length transcriptome assembly from RNA-Seq data without a reference genome. *Nature biotechnology* **29**, 644–652 (2011).
35. Haas, B. J. *et al.* *De novo* transcript sequence reconstruction from RNA-seq using the Trinity platform for reference generation and analysis. *Nature protocols* **8**, 1494–1512 (2013).
36. Haas, B. J. *et al.* Automated eukaryotic gene structure annotation using EVidenceModeler and the Program to Assemble Spliced Alignments. *Genome biology* **9**, 1–22 (2008).
37. Database resources of the national center for biotechnology information. *Nucleic acids research* **46**, D8–D13 (2018).
38. Boeckmann, B. *et al.* The SWISS-PROT protein knowledgebase and its supplement TrEMBL in 2003. *Nucleic acids research* **31**, 365–370 (2003).
39. Buchfink, B., Xie, C. & Huson, D. H. Fast and sensitive protein alignment using DIAMOND. *Nature methods* **12**, 59–60 (2015).
40. Cantalapiedra, C. P., Hernández-Plaza, A., Letunic, L., Bork, P. & Huerta-Cepas, J. eggNOG-mapper v2: functional annotation, orthology assignments, and domain prediction at the metagenomic scale. *Molecular biology and evolution* **38**, 5825–5829 (2021).
41. Kotera, M., Hirakawa, M., Tokimatsu, T., Goto, S. & Kanehisa, M. The KEGG databases and tools facilitating omics analysis: latest developments involving human diseases and pharmaceuticals. *Next Generation Microarray Bioinformatics: Methods and Protocols*, 19–39 (2012).
42. Ashburner, M. *et al.* Gene ontology: tool for the unification of biology. *Nature genetics* **25**, 25–29 (2000).
43. Mistry, J. *et al.* Pfam: The protein families database in 2021. *Nucleic acids research* **49**, D412–D419 (2021).
44. Sun, J. *et al.* OrthoVenn3: an integrated platform for exploring and visualizing orthologous data across genomes. *Nucleic acids research* **51**, W397–W403 (2023).
45. Li, C.-Y. *et al.* The sage genome provides insight into the evolutionary dynamics of diterpene biosynthesis gene cluster in plants. *Cell reports* **40** (2022).
46. Edgar, R. C. Muscle5: High-accuracy alignment ensembles enable unbiased assessments of sequence homology and phylogeny. *Nature Communications* **13**, 6968 (2022).
47. Capella-Gutiérrez, S., Silla-Martínez, J. M. & Gabaldón, T. trimAl: a tool for automated alignment trimming in large-scale phylogenetic analyses. *Bioinformatics* **25**, 1972–1973 (2009).
48. Price, M. N., Dehal, P. S. & Arkin, A. P. FastTree 2—approximately maximum-likelihood trees for large alignments. *PLoS one* **5**, e9490 (2010).
49. NCBI Sequence Read Archive <https://identifiers.org/ncbi/insdc.sra:SRP510693> (2024).
50. NCBI Sequence Read Archive <https://identifiers.org/ncbi/insdc.sra:SRX24744566> (2024).
51. NCBI Sequence Read Archive <https://identifiers.org/ncbi/insdc.sra:SRX24744567> (2024).
52. NCBI Sequence Read Archive <https://identifiers.org/ncbi/insdc.sra:SRX24744565> (2024).
53. NCBI Sequence Read Archive <https://identifiers.org/ncbi/insdc.sra:SRX24744564> (2024).
54. NCBI GenBank https://identifiers.org/ncbi/insdc.gca:GCA_041430365.1 (2024).
55. Choi, sehyun *Salvia sclarea* annotation. *figshare*. <https://doi.org/10.6084/m9.figshare.27002593.v1> (2024).

Acknowledgements

This work was supported by the National Research Foundation of Korea (NRF) grant funded by the Korean government (MSIT, No. 2022R1A2C1004127).

Author contributions

S Choi, and C Kim conceptualized and designed this study. S Choi collected the samples and conducted the experiments. S Choi, and Y Kang analyzed the data. C Kim supervised the research. S Choi wrote the draft manuscript. C Kim provided critical feedback and helped shape the research, analysis, and manuscript. Both S Choi and C Kim contributed to the final version of the manuscript. All authors read and approved the final manuscript.

Competing interests

The authors declare no competing interests.

Additional information

Correspondence and requests for materials should be addressed to C.K.

Reprints and permissions information is available at www.nature.com/reprints.

Publisher's note Springer Nature remains neutral with regard to jurisdictional claims in published maps and institutional affiliations.



Open Access This article is licensed under a Creative Commons Attribution-NonCommercial-NoDerivatives 4.0 International License, which permits any non-commercial use, sharing, distribution and reproduction in any medium or format, as long as you give appropriate credit to the original author(s) and the source, provide a link to the Creative Commons licence, and indicate if you modified the licensed material. You do not have permission under this licence to share adapted material derived from this article or parts of it. The images or other third party material in this article are included in the article's Creative Commons licence, unless indicated otherwise in a credit line to the material. If material is not included in the article's Creative Commons licence and your intended use is not permitted by statutory regulation or exceeds the permitted use, you will need to obtain permission directly from the copyright holder. To view a copy of this licence, visit <http://creativecommons.org/licenses/by-nc-nd/4.0/>.

© The Author(s) 2025